RESEARCH PAPER

Design, Optimisation, and Evaluation of Triple-Layer Sustained-Release Matrix Tablets for Co-Delivery of Diclofenac Sodium and Chondroitin Sulphate in Osteoarthritis Management

Middipoka Keerthi[1], K. E. Sailaja[2], A. Mounika[3*]

[1]Student, Department of Pharmaceutics, JNTUA–Oil Technological & Pharmaceutical Research Institute (JNTUA–OTPRI), Anantapur, Andhra Pradesh, India.
[2]Assistant Professor, Department of Pharmaceutics, JNTUA–Oil Technological & Pharmaceutical Research Institute (JNTUA–OTPRI), Anantapur, Andhra Pradesh, India.
[3]Assistant Professor, Department of Pharmacology, JNTUA–Oil Technological & Pharmaceutical Research Institute (JNTUA–OTPRI), Anantapur, Andhra Pradesh, India.

CorrespondingAuthor:
A. Mounika
Email:ID: sathish1981rs@gmail.com

ABSTRACT

Background: Osteoarthritis (OA) requires long-term co-administration of chondroitin sulphate (CTN) and diclofenac sodium (DFC). Conventional immediate-release forms cause high dosing frequency, plasma fluctuations, and significant GI side effects. **Objective:** To design and optimize a once-daily triple-layer sustained-release matrix tablet for CTN (300 mg) and DFC (150 mg) using HPMC K4M and guar gum as rate-controlling polymers. **Methods:** Nine formulations (F1–F9) were prepared via central composite design (RSM). HPMC K4M and guar gum were optimized against cumulative drug release (%CDR) and swelling index. Dissolution (USP II, pH 6.8, 12 h), release kinetics, and accelerated stability (40°C/75% RH, 90 days, ICH guidelines) were evaluated. **Results:** All formulations met pharmacopeial standards. Optimized F7 (HPMC K4M 450 mg, guar gum 387.84 mg) achieved 12-hour dual sustained release via non-Fickian anomalous transport ($n = 0.6968$). The RSM quadratic model for %CDR showed excellent fit (Adj. $R^2 = 0.9997$, $p < 0.0001$), with HPMC K4M as the dominant rate-controlling polymer. Drug content: DFC 98.02%, CTN 98.95%. F7 remained stable over 90 days. **Conclusion:** The optimized triple-layer matrix F7 enables once-daily co-sustained release of CTN and DFC for OA, offering improved patient adherence, reduced GI toxicity, and a scalable platform combining disease-modifying and anti-inflammatory therapy.

Keywords: *Triple-layer matrix tablet; Chondroitin sulphate; Diclofenac sodium; HPMC K4M; Guar gum; Response surface methodology*

How to cite this article: Keerthi M, Sailaja KE, Mounika A. Design, Optimisation, and Evaluation of Triple-Layer Sustained-Release Matrix Tablets for Co-Delivery of Diclofenac Sodium and Chondroitin Sulphate in Osteoarthritis Management. Int J Drug Deliv Technol. 2026;16(62s): 978-996. DOI: 10.25258/ijddt.16.62s.105

Source of support: Nil.
Conflict of interest: Nil.

INTRODUCTION

Osteoarthritis (OA) is the most prevalent musculoskeletal disorder worldwide, characterised by progressive degradation of articular cartilage, synovial inflammation, periarticular bone remodelling, and loss of joint function [1,2]. Its global burden is expected to escalate substantially with population ageing, imposing enormous socioeconomic costs. The pharmacological cornerstone of OA management involves two mechanistically distinct agents: chondroitin sulphate (CTN), a disease-modifying symptomatic slow-acting drug (SYSADOA), and diclofenac sodium (DFC), a potent non-steroidal anti-inflammatory drug (NSAID) [3,4].

CTN is a sulphated glycosaminoglycan (GAG) that constitutes a fundamental structural component of articular cartilage. It exerts chondroprotective effects through anti-inflammatory activity, stimulation of proteoglycan and hyaluronic acid synthesis, and inhibition of catabolic enzymes (metalloproteinases) responsible for cartilage degradation [3,5,26]. Its oral bioavailability ranges from 15–24% with a plasma half-life of 6 hours, and a recommended dose of 800–1200 mg/day [5,79]. DFC, a phenylacetic acid-derived NSAID with a plasma half-life of 1.5–2.0 hours, exerts potent analgesic and anti-inflammatory activity by inhibiting COX-1 and COX-2 enzymes, thereby suppressing prostaglandin biosynthesis [6,7,18,81]. Chronic oral DFC at therapeutic doses (75–150 mg/day)

**Author for Correspondance:* sathish1981rs@gmail.com

carries significant GI risks including mucosal irritation, peptic ulceration, and cardiovascular complications [6,7,9].

Conventional IR formulations of both drugs necessitate multiple daily dosing, imposing plasma level fluctuations, dosing inconvenience, reduced long-term adherence, and dose-dependent adverse effects. SR oral matrix systems represent an established strategy to overcome these limitations by prolonging drug release and stabilising plasma concentrations [10,13,16]. Hydrophilic matrix tablets incorporating HPMC K4M and natural polysaccharides such as guar gum achieve controlled release through viscous gel layer formation upon hydration, modulating drug diffusion and matrix erosion simultaneously [11,14,67].

Triple-layer matrix tablets provide a structural advantage over single-layer matrices: the active drug core is flanked by two outer polymeric retardant layers, providing bilateral release modulation, structural protection against dose dumping, and independent control of polymer concentrations [14,16]. Response Surface Methodology (RSM) enables rational multi-factor optimisation with fewer experimental runs, capturing non-linear relationships between formulation variables and performance responses [12].

Despite extensive literature on SR DFC formulations [20,21,22,24] and CTN delivery systems [25,29,40], no published study has reported an RSM-optimised triple-layer matrix co-delivering both CTN and DFC for OA. The present study aimed to: (i) design triple-layer matrix tablets co-delivering CTN (300 mg) and DFC (150 mg); (ii) optimise HPMC K4M and guar gum concentrations using RSM central composite design against %CDR and SI; (iii) comprehensively evaluate physicochemical, dissolution, kinetic, and stability profiles; and (iv) elucidate the drug release mechanism to validate the system as a once-daily OA treatment platform.

Materials and Methods

Materials

Chondroitin sulphate (CTN; Balaji Drugs), diclofenac sodium (DFC; Orbit Pharma Laboratories), HPMC E5 LV and K4M (Loba Chemi Pvt. Ltd.), guar gum (Loba Chemi Pvt. Ltd.), lactose (Loba Chemi Pvt. Ltd.), PVP K-30 (Loba Chemi Pvt. Ltd.), isopropyl alcohol (Loba Chemi Pvt. Ltd.), magnesium stearate (SD Fine Chem Ltd.), and talc (Central Drug House Pvt. Ltd.) were used as received. All reagents and solvents were of analytical or pharmacopoeial grade.

Preformulation Studies

Organoleptic Evaluation and Melting Point Determination

CTN and DFC were evaluated for colour, odour, texture, and taste. Melting point of CTN was determined using the capillary method and confirmed by DSC [69]. UV spectra of both drugs were recorded over 200–400 nm in PBS pH 6.8 to identify the isobestic point for simultaneous quantification [74].

Standard Calibration Curves

Standard solutions of CTN and DFC (10–60 µg/mL) were prepared in PBS pH 6.8. UV absorbance was recorded using a UV-1800 double-beam spectrophotometer (Shimadzu, Japan). The isobestic point—where absorbances of both compounds are equal independent of their individual concentrations—was identified at 276 nm. Calibration curves (absorbance vs. concentration) were constructed; linearity was assessed by R^2 [74].

Differential Scanning Calorimetry (DSC)

DSC was performed on pure CTN, pure DFC, and binary drug–excipient mixtures (1:1 w/w) using a Bruker DSC at 10°C/min from 30–250°C under nitrogen (50 mL/min). Endothermic peak temperatures and enthalpies were recorded and compared to detect thermal interactions indicating incompatibility [69].

FTIR Spectroscopy

FTIR analysis of pure CTN, pure DFC, and their excipient mixtures was performed on a Bruker FTIR spectrometer (KBr pellets, 4000–400 cm^{-1}). Characteristic absorption bands were identified, and any new peaks, peak disappearances, or significant wavenumber shifts in mixture spectra were noted as evidence of chemical interaction [69].

Experimental Design: Response Surface Methodology

A central composite design (CCD) under RSM was employed using Design Expert® v13 (Stat-Ease Inc.) with HPMC K4M (Factor A) and guar gum (Factor B) as independent variables. Nine formulations (F1–F9) were generated per the design matrix with %CDR and SI as responses. Polynomial models (linear, 2FI, quadratic) were fitted; selection was based on statistical significance (F-test, $p < 0.05$), adjusted R^2, predicted R^2, and lack-of-fit test [12].

Formulation of Triple-Layer Matrix Tablets

Nine triple-layer formulations (F1–F9) were prepared by wet granulation. Each tablet comprised three layers compressed sequentially: (i) upper retardant layer – HPMC K4M granules; (ii) middle active core – CTN (300 mg) + DFC (150 mg) granules; (iii) lower retardant layer guar gum granules. Composition is detailed in Table 1. Each

layer was granulated separately using isopropyl alcohol (qs), dried at 50 ± 2°C for 2 h, sieved through #20 mesh, and lubricated with magnesium stearate (150 mg) and talc (150 mg). Triple-layer tablets were compressed

on a multi-station machine (Lab India) to a target total weight of ~2.22 g [14].

Table 1. Composition of triple-layer matrix tablet formulations F1–F9 (amounts in mg per tablet).

Ingredient (mg)	F1	F2	F3	F4	F5	F6	F7	F8	F9
Chondroitin Sulphate	300	300	300	300	300	300	300	300	300
Diclofenac Sodium	150	150	150	150	150	150	150	150	150
HPMC K4M (Factor A)	300	600	300	600	237.84	662.10	450	450	450
Guar Gum (Factor B)	450	450	750	750	600	600	387.84	812.13	600
Lactose	690	390	390	90	602.16	177.90	602.16	177.87	390
PVP K-30	30	30	30	30	30	30	30	30	30
Isopropyl Alcohol	qs	qs	qs	qs	qs	qs	qs	qs	qs
Magnesium Stearate	150	150	150	150	150	150	150	150	150
Talc	150	150	150	150	150	150	150	150	150
Total Weight (mg)	2220	2220	2220	2220	2220	2220	2220	2220	2220

F7 (green) = optimised formulation. HPMC = hydroxypropyl methylcellulose; PVP = polyvinylpyrrolidone; qs = sufficient quantity (evaporated during drying). Factor A = HPMC K4M; Factor B = guar gum (RSM independent variables).

Pre-Compression Evaluation

Granule blends were characterised for angle of repose (fixed funnel method), bulk density (ρb), tapped density (ρt), Carr's Index [CI = (ρt − ρb)/ρt × 100], and Hausner's Ratio [HR = ρt/ρb]. Measurements in triplicate (n = 3) [71].

Post-Compression Evaluation

Tablets were evaluated for thickness (Vernier calliper, n = 5), hardness (Pfizer tester, n = 5), weight variation (n = 20; USP ± 5%), friability (Roche friabilator, 25 rpm, 100 rev., n = 10; < 1%), drug content uniformity (CTN and DFC, n = 5; 85–115% LC), and disintegration time (USP Type I, n = 6) [72,74].

Swelling Index (SI)

Tablets (W_0) were placed in PBS pH 7.2 (25 mL). At 1-hour intervals over 12 hours, tablets were removed, blotted, and reweighed (Wt). SI (%) = [(Wt − W_0)/W_0] × 100. n = 3.

In-Vitro Drug Release Studies

USP Type II paddle apparatus (Lab India DS 8000), 900 mL PBS pH 6.8, 37 ± 0.5°C, 75 rpm, 12 hours (n = 3). Aliquots (5 mL) withdrawn hourly, replaced with fresh medium. Samples filtered (0.45 µm), analysed at 276 nm (isobestic point) [74]. %CDR calculated from pre-validated calibration curves.

Drug Release Kinetics

Release data were fitted to zero-order, first-order, Higuchi, Hixson–Crowell, and Korsmeyer–Peppas [Mt/M∞ = kt^n] models. Best fit selected by highest correlation coefficient (r). Korsmeyer–Peppas n value: < 0.5 = quasi-Fickian; = 0.5 = Fickian; 0.5–1.0 = non-Fickian (anomalous); = 1.0 = Case-II transport [75].

RSM Statistical Analysis

Quadratic models for %CDR and SI were evaluated by ANOVA (F-test, $p < 0.05$), adjusted R^2, lack-of-fit, and residual diagnostics (normal probability plot, residuals vs. run, predicted vs. actual, Cook's distance). Contour and 3D response surface plots were generated. $p < 0.05$ = significant [12].

Accelerated Stability Studies

F7 was stored in Alu–Alu blisters at 40 ± 2°C/75 ± 5% RH for 90 days (ICH Q1A R2). Samples withdrawn at days 0, 30, 60, 90 and evaluated for appearance, weight variation, hardness, friability, disintegration time, moisture content, drug content (CTN and DFC), and in-vitro drug release [12].

Results

3.1 Preformulation Studies

3.1.1 Organoleptic Properties and Triple-Layer Architecture

Both CTN and DFC appeared as white-to-off-white crystalline powders with characteristic odours. Melting point of CTN was 158.3°C (pharmacopoeial range: 156–162°C), confirming identity and purity [69]. The triple-layer tablets exhibited a biconvex oval geometry with three clearly distinguishable layers visible on cross-section, smooth surfaces, no cracks or chips, and good inter-layer adhesion, confirming successful sequential compression (Figure 1) [69].

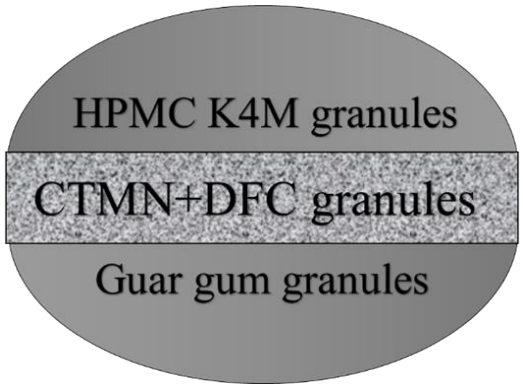

Figure 1. Schematic cross-section of the triple-layer matrix tablet (Fig. 5.1 from thesis): upper HPMC K4M retardant layer, middle CTN+DFC active drug core, and lower guar gum retardant layer. Arrows indicate hydration-driven gel front and drug diffusion pathways.

3.1.2 Standard Calibration Curves

Simultaneous UV quantification of CTN and DFC at the isobestic point (276 nm, PBS pH 6.8) demonstrated excellent linearity across 10–60 µg/mL (Table 2, Figure 2). Regression equations: CTN: $y = 0.0093x + 0.0727$ ($R^2 = 0.9964$); DFC: $y = 0.0105x + 0.1479$ ($R^2 = 0.9995$), confirming method suitability for dissolution analysis [74].

Table 2. Calibration curve data for CTN and DFC at isobestic point (276 nm, PBS pH 6.8).

Concentration (µg/mL)	CTN Absorbance	DFC Absorbance
10	0.156	0.251
20	0.258	0.364
30	0.365	0.458
40	0.456	0.569
50	0.526	0.668
60	0.628	0.781
Regression Equation	y = 0.0093x + 0.0727	y = 0.0105x + 0.1479
R^2	0.9964	0.9995

CTN = chondroitin sulphate; DFC = diclofenac sodium. n = 3, mean values reported.

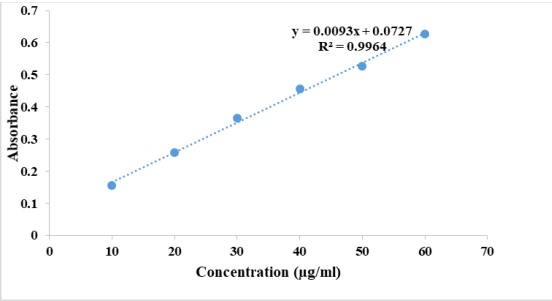

Figure 2. Calibration curves for CTN (left) and DFC (right) at isobestic point 276 nm in PBS pH 6.8 ($R^2 > 0.996$ for both, confirming linearity across 10–60 µg/mL).

3.1.3 DSC Studies

Pure CTN showed a sharp endothermic peak at Tpeak = 159.06°C (Tonset = 148.81°C; ΔH = −487.13 J/g), confirming its crystalline nature. In the CTN–excipient mixture, the peak shifted to 125.38°C (Tonset = 110.36°C; ΔH = −395.77 J/g), indicating partial amorphisation and physical interaction with excipients. No new exothermic events were detected, confirming absence of chemical incompatibility (Figure 3a) [69].

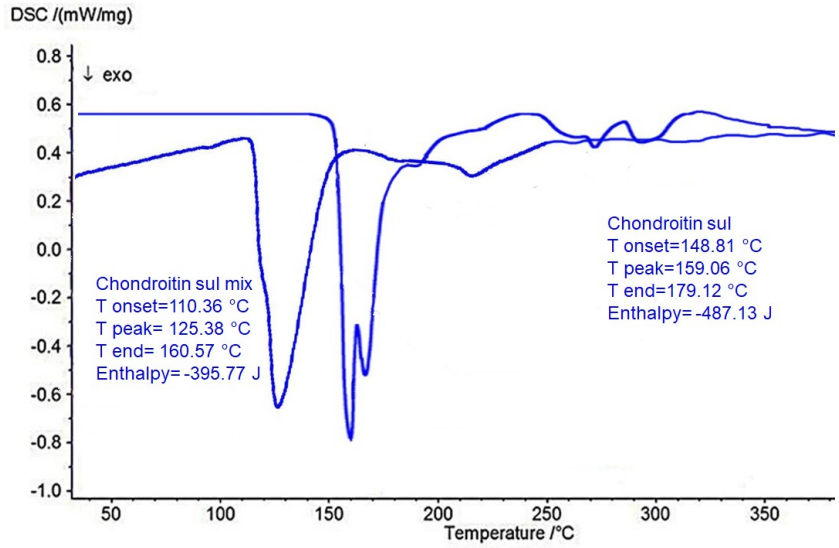

Figure 3a. DSC thermogram of pure chondroitin sulphate (CTN) and CTN–excipient binary mixture. Shift in onset temperature (148.81°C → 110.36°C) indicates partial amorphisation without chemical degradation.

Pure DFC showed a sharp endotherm at Tpeak = 160.14°C (ΔH = −547.08 J/g). In the DFC–excipient mixture, Tonset shifted to 111.25°C (Tpeak = 151.99°C; ΔH = −611.64 J/g). The broadened, lowered endotherm reflects increased amorphous content, potentially enhancing dissolution. No new peaks or decomposition events confirmed physicochemical compatibility (Figure 3b) [69].

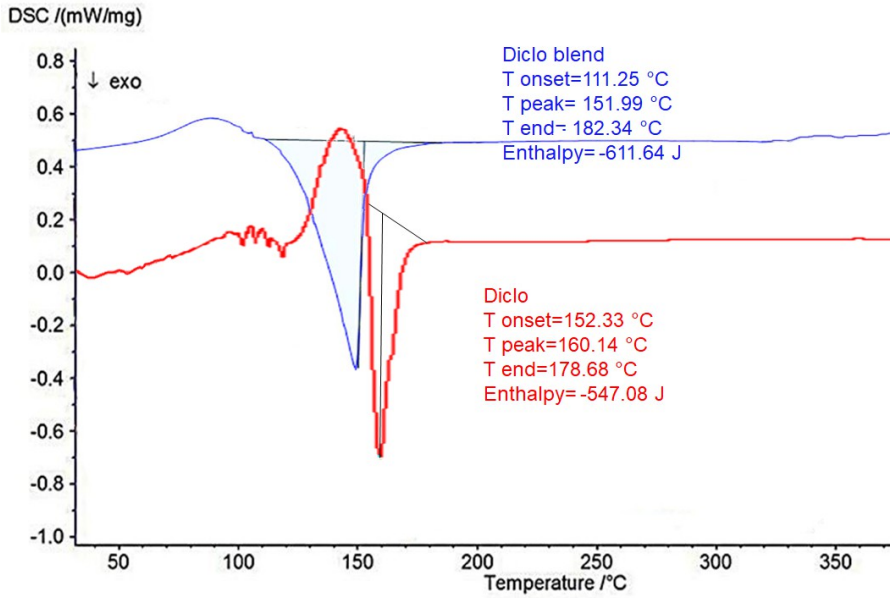

Figure 3b. DSC thermogram of pure diclofenac sodium (DFC) and DFC–excipient binary mixture. Lowered onset temperature (160.14°C → 111.25°C) indicates increased amorphous content; no chemical incompatibility observed.

*Author for Correspondance: sathish1981rs@gmail.com

3.1.4 FTIR Spectroscopy

FTIR spectrum of pure CTN exhibited characteristic bands: broad O–H/N–H stretching (~3300 cm^{-1}), sulphate S=O asymmetric stretching (~1240 cm^{-1}), glycosidic C–O–C (~1650–1000 cm^{-1}), and C–O–S (~850 cm^{-1}). All characteristic peaks were fully preserved in the CTN–excipient mixture with no new absorptions or significant shifts, confirming physicochemical compatibility (Figure 4a) [69].

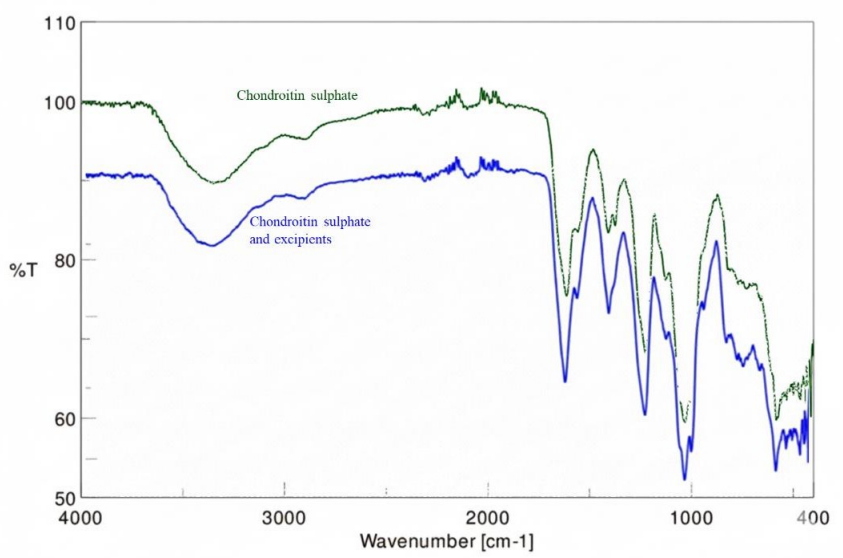

Figure 4a. FTIR spectra of pure CTN (green) and CTN–excipient mixture (blue). All characteristic bands retained without new peaks, confirming chemical compatibility.

FTIR spectrum of pure DFC showed characteristic bands at ~3380 cm^{-1} (N–H stretching), ~1575 cm^{-1} (asymmetric COO^-), ~1440 cm^{-1} (symmetric COO^-), and ~760 cm^{-1} (C–Cl stretching). All peaks were retained in the DFC–excipient mixture, confirming chemical stability of DFC in the presence of all proposed excipients (Figure 4b) [69].

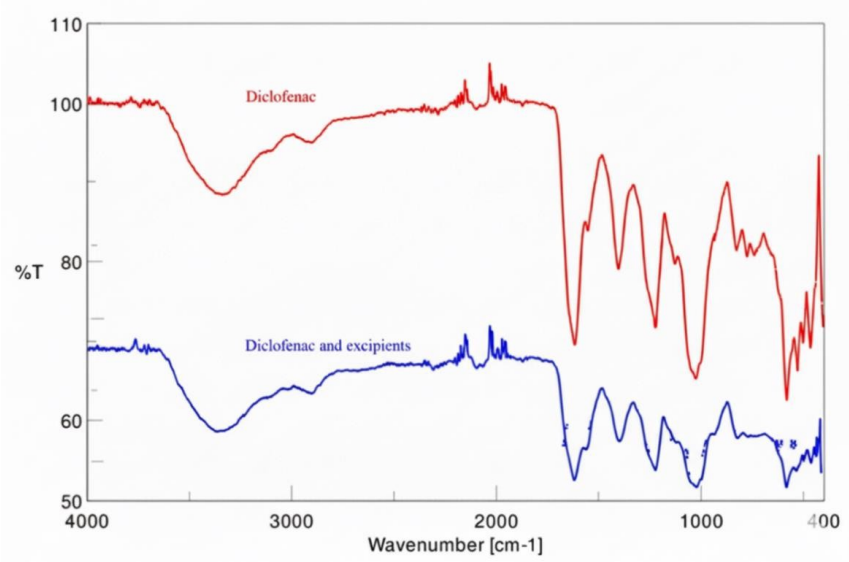

Figure 4b. FTIR spectra of pure DFC (green) and DFC–excipient mixture (blue). Retention of all functional group bands confirms drug–excipient chemical compatibility.

3.2 Pre-Compression Evaluation

Pre-compression flow properties for all nine formulations are presented in Table 3. Angle of repose ranged from 26.5 ± 0.8° (F6) to 29.0 ± 0.5° (F4), all below 30°, indicating excellent flowability. Carr's Index (9.0–10.2%) and Hausner's Ratio (~1.10–1.11) confirmed excellent powder compressibility, validating suitability for tableting [71].

Table 3. Pre-compression flow properties of granule blends F1–F9 (mean ± SD, n = 3).

Form.	Angle of Repose (°)	Bulk Density (g/mL)	Tapped Density (g/mL)	Carr's Index (%)	Hausner's Ratio	Flow Class
F1	27.3 ± 0.5	0.45 ± 0.01	0.50 ± 0.01	10.0 ± 0.5	1.11 ± 0.01	Excellent
F2	28.1 ± 0.4	0.47 ± 0.02	0.52 ± 0.02	9.0 ± 0.2	1.11 ± 0.04	Excellent
F3	26.8 ± 0.8	0.46 ± 0.02	0.51 ± 0.03	9.8 ± 0.5	1.11 ± 0.02	Excellent
F4	29.0 ± 0.5	0.44 ± 0.01	0.49 ± 0.03	10.2 ± 0.4	1.11 ± 0.03	Excellent
F5	27.5 ± 0.4	0.48 ± 0.02	0.53 ± 0.02	9.4 ± 0.1	1.10 ± 0.01	Excellent
F6	26.5 ± 0.8	0.46 ± 0.03	0.51 ± 0.01	9.8 ± 0.4	1.11 ± 0.01	Excellent
F7	28.3 ± 0.4	0.45 ± 0.01	0.50 ± 0.04	10.0 ± 0.2	1.11 ± 0.06	Excellent
F8	27.0 ± 0.7	0.47 ± 0.03	0.52 ± 0.01	9.6 ± 0.4	1.11 ± 0.01	Excellent
F9	26.9 ± 0.4	0.46 ± 0.01	0.51 ± 0.02	9.8 ± 0.5	1.11 ± 0.09	Excellent

F7 (green) = optimised formulation. Flow classification per pharmacopeial guidelines [71]: Carr's Index < 10% = Excellent; HR 1.00–1.11 = Excellent.

3.3 Post-Compression Evaluation

Post-compression parameters for all formulations are shown in Table 4. Tablet thickness (3.62–3.94 mm), hardness (5.7–7.2 kg/cm²), friability (0.25–0.81%, all < 1%), weight variation (1.08–1.95%), and drug content (DFC: 93.65–98.02%; CTN: 94.09–98.95%) all satisfied pharmacopeial acceptance criteria [72,74]. F7 showed the highest drug contents (DFC: 98.02 ± 3.51%; CTN: 98.95 ± 3.54%), confirming excellent granule mixing uniformity.

Table 4. Post-compression physicochemical parameters of triple-layer matrix tablets F1–F9 (mean ± SD).

Form.	Thickness (mm) n=5	Hardness (kg/cm²) n=5	Wt. Variation (%) n=20	Friability (%) n=10	DFC Content (%) n=5	CTN Content (%) n=5	Result
F1	3.81 ± 0.12	5.9 ± 0.12	1.52 ± 0.03	0.51 ± 0.01	95.82 ± 1.25	94.09 ± 2.02	Pass
F2	3.62 ± 0.09	6.1 ± 0.35	1.62 ± 0.04	0.36 ± 0.02	95.62 ± 3.02	95.27 ± 3.05	Pass
F3	3.94 ± 0.07	5.8 ± 0.02	1.35 ± 0.02	0.25 ± 0.03	96.34 ± 2.35	97.02 ± 3.15	Pass
F4	3.88 ± 0.08	6.8 ± 0.14	1.72 ± 0.04	0.71 ± 0.01	94.02 ± 3.60	96.35 ± 4.12	Pass
F5	3.75 ± 0.15	6.3 ± 0.24	1.48 ± 0.03	0.58 ± 0.04	97.86 ± 0.18	95.06 ± 2.07	Pass
F6	3.68 ± 0.05	5.7 ± 0.08	1.22 ± 0.02	0.64 ± 0.05	93.65 ± 2.84	94.12 ± 1.65	Pass
F7	3.81 ± 0.03	6.3 ± 0.07	1.62 ± 0.01	0.81 ± 0.03	98.02 ± 3.51	98.95 ± 3.54	Pass

F8	3.92 ± 0.01	6.9 ± 0.14	1.95 ± 0.02	0.46 ± 0.01	94.72 ± 1.65	96.34 ± 2.15	Pass
F9	3.68 ± 0.02	7.2 ± 0.22	1.08 ± 0.01	0.38 ± 0.02	97.36 ± 2.06	95.12 ± 4.11	Pass
Acceptance Limits	—	5–8 kg/cm²	≤ ±5%	< 1%	85–115% LC	85–115% LC	—

F7 (green) = optimised formulation. LC = label claim. DFC = diclofenac sodium; CTN = chondroitin sulphate.

3.4 Swelling Index

Swelling index at 12 hours ranged from ~50% (F6) to ~69% (F7) (Figure 5). F7 (intermediate HPMC K4M 450 mg; GG 387.84 mg) showed the highest SI, reflecting robust, balanced gel-layer formation optimal for sustained diffusion-controlled release. F6 (highest HPMC K4M at 662.10 mg) showed the lowest SI, consistent with dense gel restricting water penetration—a finding confirmed by the RSM analysis (Section 3.7.2). Progressive swelling over 12 hours was observed for all formulations, confirming adequate matrix structural integrity.

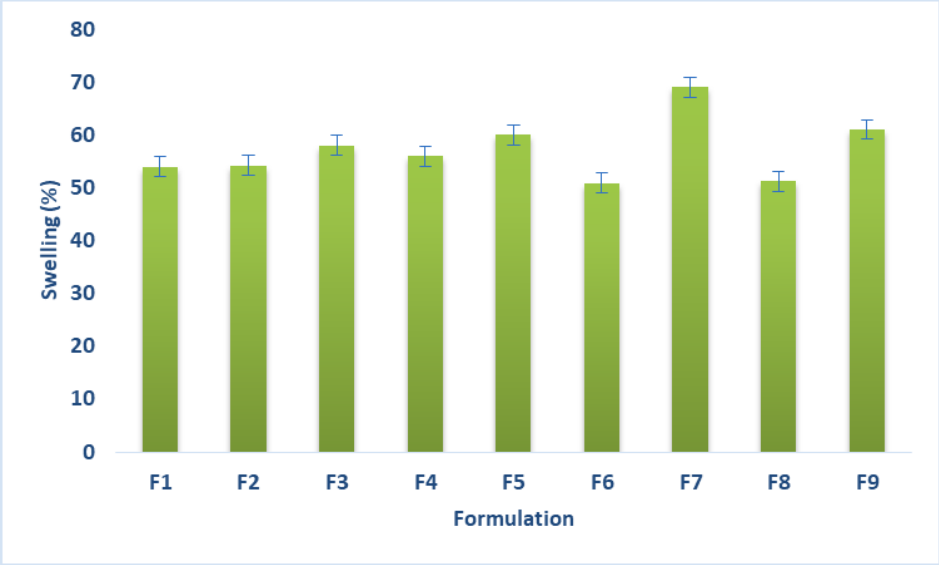

Figure 5. Comparative swelling index (%) at 12 hours in PBS pH 7.2 for formulations F1–F9 (mean ± SD, n = 3). F7 showed maximum swelling (69%), consistent with optimal hydrophilic matrix behaviour for sustained drug release.

3.5 In-Vitro Drug Release Studies

In-vitro dissolution profiles for CTN and DFC from all nine formulations over 12 hours are presented in Figures 6a and 6b. All formulations demonstrated genuine, smooth sustained release with no burst effect, confirming the effectiveness of the triple-layer polymer matrix architecture in preventing dose dumping.

For CTN: cumulative release at 12 h ranged from ~82% (F4, F8, F9) to ~100% (F5, F7). F7 produced the most complete and consistent CTN release profile (~98% at 12 h). For DFC: F1 showed the fastest release (~100% at 12 h) due to its lower guar gum content combined with moderate HPMC K4M. F4, F6, and F9 showed the most retarded DFC release (~80–90% at 12 h) attributable to high combined polymer concentrations. F7 produced consistent, reproducible DFC sustained release (~95% at 12 h) with a smooth, zero-order-like profile [20,22,24,39].

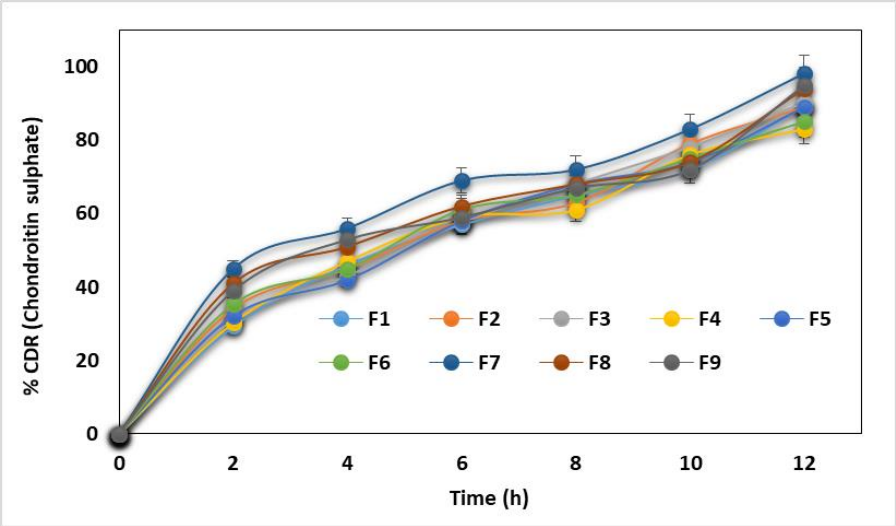

Figure 6a. In-vitro cumulative drug release of chondroitin sulphate (CTN) from formulations F1–F9 in PBS pH 6.8 over 12 hours (USP Type II, 75 rpm, 37°C; n = 3, mean ± SD). F7 (optimised) showed ~98% CDR with smooth, sustained profile.

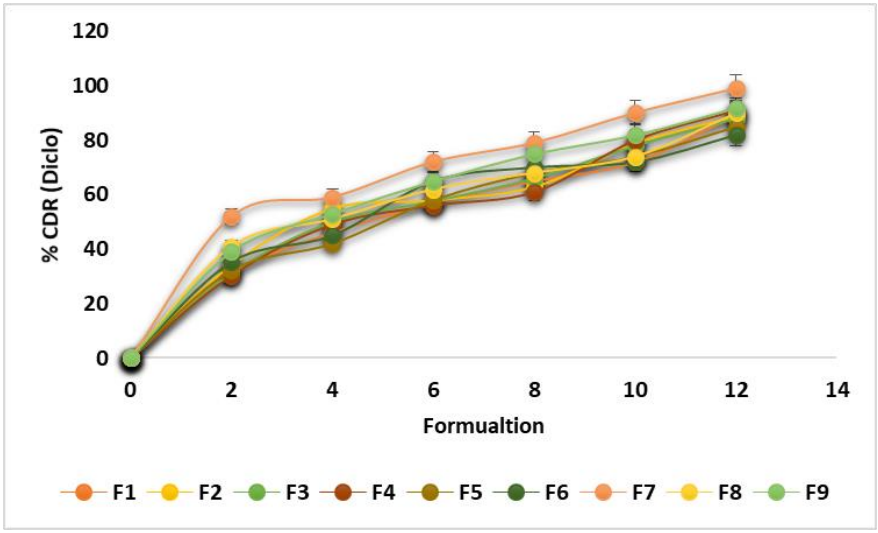

Figure 6b. In-vitro cumulative drug release of diclofenac sodium (DFC) from formulations F1–F9 in PBS pH 6.8 over 12 hours (n = 3, mean ± SD). F7 showed ~95% CDR; formulations with higher polymer concentrations (F4, F6, F9) showed most retarded profiles.

3.6 Drug Release Kinetics

Release kinetics modelling results are presented in Table 5. Zero-order (r = 0.9527–0.9948) provided the highest correlation for all formulations, confirming concentration-independent, constant-rate drug release characteristic of effective SR systems. Higuchi model fits (r = 0.9147–0.9605) confirmed diffusion-mediated release. Korsmeyer–Peppas exponent n ranged from 0.5256 (F1) to 0.6968 (F7), all within $0.5 < n < 1.0$, confirming non-Fickian (anomalous) transport—drug release governed simultaneously by Fickian diffusion and polymer chain relaxation/erosion [75]. F7 showed the highest n value (0.6968), indicating the strongest erosion-diffusion combination, mechanistically consistent with the triple-layer architecture [13,15,39].

Table 5. Drug release kinetic model correlation coefficients (r) and Korsmeyer–Peppas exponent (n) for F1–F9.

Form.	Zero-Order r	First-Order r	Higuchi r	Hixson–Crowell r	Korsmeyer–Peppas r	n	Mechanism
F1	0.9851	0.9102	0.9605	0.9258	0.7948	0.5256	Non-Fickian
F2	0.9948	0.9215	0.9515	0.9345	0.7785	0.6154	Non-Fickian
F3	0.9718	0.9358	0.9454	0.9626	0.7706	0.6281	Non-Fickian
F4	0.9654	0.9457	0.9147	0.9544	0.7416	0.6329	Non-Fickian
F5	0.9746	0.9259	0.9326	0.9365	0.8472	0.6475	Non-Fickian
F6	0.9527	0.9384	0.9524	0.9257	0.7235	0.6635	Non-Fickian
F7	0.9623	0.9413	0.9232	0.9325	0.8168	0.6968	Non-Fickian
F8	0.9815	0.9045	0.9419	0.9208	0.8027	0.6262	Non-Fickian
F9	0.9874	0.9555	0.9355	0.9002	0.8568	0.6558	Non-Fickian

Non-Fickian (anomalous): 0.5 < n < 1.0 — combined diffusion and polymer relaxation/erosion. F7 = optimised (green). r = correlation coefficient [75].

3.7 RSM Optimisation – Response 1: Cumulative Drug Release (%CDR)

3.7.1 Fit Summary

The fit summary for %CDR (Table 6) showed the linear model was significant ($p < 0.0001$; Adj. $R^2 = 0.9601$). The 2FI model did not improve fit ($p = 0.8989$), indicating no significant synergistic polymer interaction. The quadratic model was both highly significant (sequential $p = 0.0002$) and exceptionally accurate (Adj. $R^2 = 0.9997$) and was selected as the recommended model [12].

Table 6. RSM fit summary for %CDR response.

Source	Sequential p-value	Adjusted R^2	Predicted R^2
Linear	< 0.0001 *	0.9601	0.9487
2FI	0.8989	0.9522	0.9433
Quadratic ✓ Recommended	0.0002 *	0.9997	—
Cubic (aliased)	0.2827	0.9999	—

** Significant ($p < 0.05$). ✓Recommended model.*

3.7.2 ANOVA for the Quadratic Model (%CDR)

ANOVA (Table 7) confirmed the overall model was highly significant ($F = 5375.91$; $p < 0.0001$). HPMC K4M (Factor A) was the dominant contributor (SS = 105.83; $F = 25055.41$; $p < 0.0001$), accounting for ~93.2% of model SS. Guar gum (Factor B) was also significant ($F = 1021.73$; $p < 0.0001$). Quadratic terms A^2 ($p = 0.0006$) and B^2 ($p < 0.0001$) confirmed non-linear, curvature effects. The AB interaction was not significant ($p = 0.1891$), confirming additive polymer actions [12].

Table 7. ANOVA for the quadratic model – %CDR response.

Source	Sum of Squares	df	Mean Square	F-value	p-value	Sig.
Model	113.53	5	22.71	5375.91	< 0.0001	***
A – HPMC K4M	105.83	1	105.83	25055.41	< 0.0001	***
B – Guar Gum	4.32	1	4.32	1021.73	< 0.0001	***
AB (interaction)	0.0121	1	0.0121	2.86	0.1891	NS
A^2 (quadratic)	0.9472	1	0.9472	224.27	0.0006	***
B^2 (quadratic)	3.32	1	3.32	785.79	< 0.0001	***
Residual	0.0127	3	0.0042	—	—	—
Corrected Total	113.54	8	—	—	—	—

**** $p < 0.001$ (highly significant); NS = not significant ($p > 0.05$). df = degrees of freedom.*

3.7.3 Polynomial Equation and Response Surfaces

$$\%CDR = +90.24 - 3.64A + 0.7345B - 0.0550AB - 0.5706A^2 - 1.07B^2$$

The negative coefficient of A (−3.64) confirms HPMC K4M strongly retards drug release. The positive coefficient of B (+0.7345) indicates moderate guar gum enhances release via swelling. The non-significant AB term (−0.0550) confirms additive polymer actions. Significant negative quadratic terms ($A^2 = -0.5706$; $B^2 = -1.07$) confirm non-linear curvature: mid-range polymer concentrations are optimal. Diagnostic plots (Figure 7) confirmed model normality, homoscedasticity, and absence of outliers. Response surface plots (Figure 8) visually confirmed HPMC K4M dominance and the optimal design space [12].

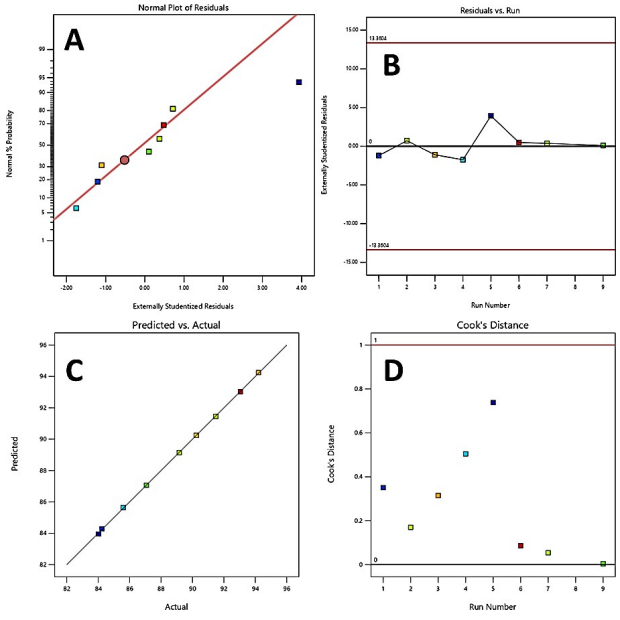

Figure 7. Diagnostic plots for the %CDR quadratic model: (A) normal probability plot of residuals – confirms normality; (B) residuals vs. run – confirms homoscedasticity; (C) predicted vs. actual – confirms model accuracy ($R^2 \approx 1.0$); (D) Cook's distance – all below 1.0, no outliers.

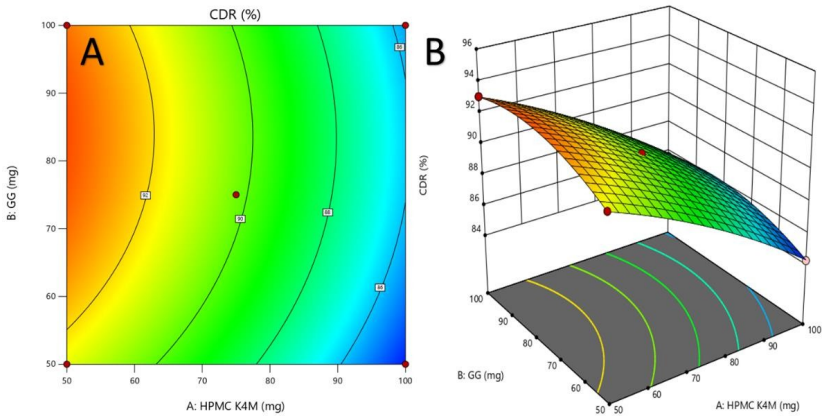

Figure 8. RSM response surface for %CDR: (A) 2D contour plot – regions of high CDR (warmer colours) shift to lower CDR as HPMC K4M increases; (B) 3D surface plot – steep decline along HPMC K4M axis confirming dominant rate-controlling role; dome shape confirms non-linear quadratic effects.

3.8 RSM Optimisation – Response 2: Swelling Index (%SI)

3.8.1 Fit Summary and ANOVA

The fit summary for %SI (Table 8) indicated the quadratic model achieved Adj. $R^2 = 0.9467$ with no significant lack of fit ($p = 0.9467$), confirming model adequacy [12]. ANOVA (Table 9) confirmed overall model significance ($F = 29.44$; $p = 0.0094$). HPMC K4M was the dominant determinant ($F = 122.13$; $p = 0.0016$), with significant quadratic term A^2 ($p = 0.0269$) confirming non-linear, concentration-dependent swelling. Guar gum and AB interaction were not significant, confirming HPMC K4M's primary role in swelling behaviour.

Table 8. RSM fit summary for %SI response.

Source	Sequential p-value	Adjusted R^2	Predicted R^2
Linear	0.0030 *	0.8069	0.7195
2FI	0.5980	0.7820	0.6690
Quadratic ✓ Suggested	0.0561	0.9467	—
Cubic (aliased)	0.2640	0.9889	—

** $p < 0.05$. Quadratic model selected: highest Adj. R^2 and non-significant lack of fit ($p = 0.9467$).*

Table 9. ANOVA for the quadratic model – %SI response.

Source	Sum of Squares	df	Mean Square	F-value	p-value	Significance
Model	146.42	5	29.28	29.44	0.0094	Significant
A – HPMC K4M	121.47	1	121.47	122.13	0.0016	**
B – Guar Gum	6.29	1	6.29	6.32	0.0866	NS
AB (interaction)	1.29	1	1.29	1.30	0.3378	NS

Source	Sum of Squares	df	Mean Square	F-value	p-value	Significance
A^2 (quadratic)	16.42	1	16.42	16.51	0.0269	*
B^2 (quadratic)	3.33	1	3.33	3.35	0.1645	NS
Residual	2.98	3	0.9947	—	—	—
Corrected Total	149.41	8	—	—	—	—

*** p < 0.01; * p < 0.05; NS = not significant (p > 0.05).*

3.8.2 Polynomial Equation and Response Surfaces

$$\%SI = +96.65 - 3.90A + 0.8867B - 0.5675AB - 2.38A^2 - 1.07B^2$$

HPMC K4M (A = −3.90) exerts the dominant inverse effect on SI through gel densification at higher concentrations. Guar gum (B = +0.8867) modestly enhances swelling. The strong negative quadratic term A^2 (−2.38) confirms maximum SI at intermediate HPMC K4M concentrations, declining at extremes. Diagnostic plots (Figure 9) and 3D response surface plots (Figure 10) confirmed model adequacy and the dominant role of HPMC K4M in determining swelling behaviour [12].

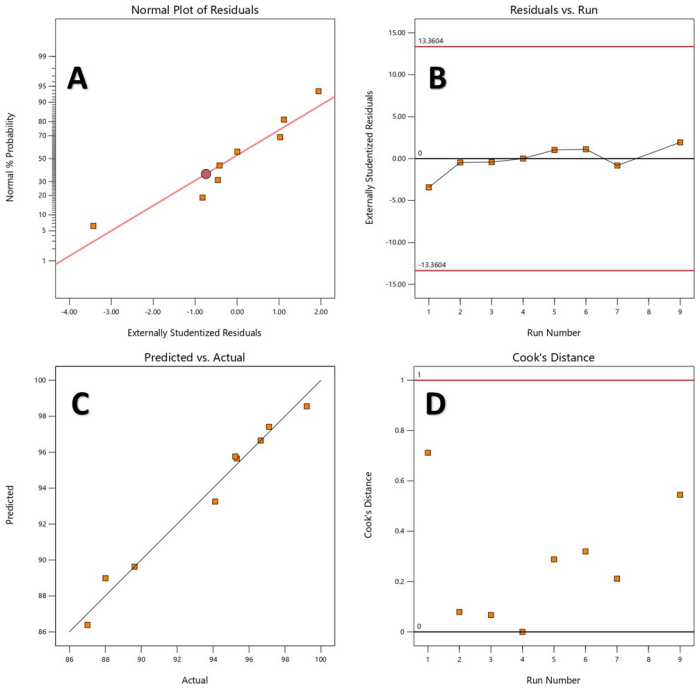

Figure 9. Diagnostic plots for the %SI quadratic model: (A) normal probability plot; (B) residuals vs. run; (C) predicted vs. actual; (D) Cook's distance. All diagnostics confirm model adequacy with no outliers.

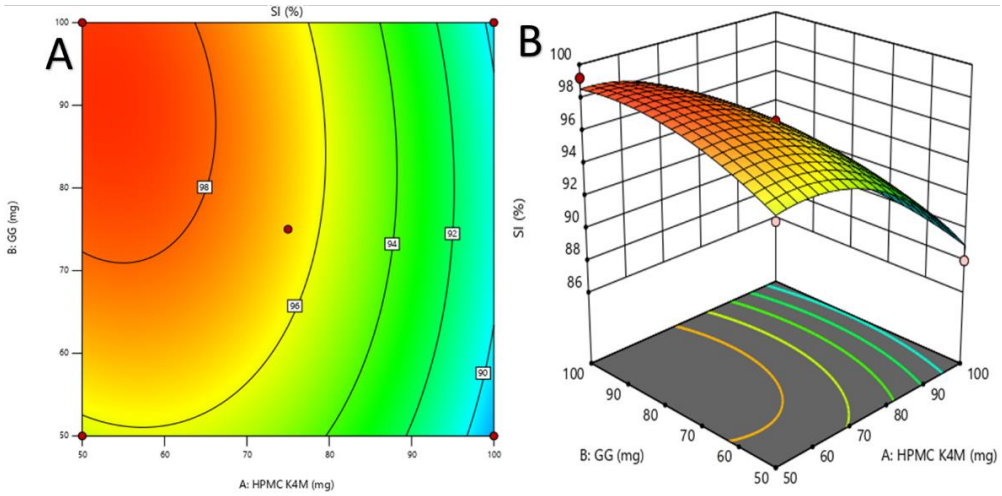

Figure 10. RSM response surface for %SI: (A) 2D contour plot showing design space for swelling index; (B) 3D surface plot – dome-shaped surface confirms non-linear, quadratic effect of HPMC K4M; maximum SI at intermediate polymer concentrations (F7 design space).

3.9 Accelerated Stability Studies

Stability data for F7 at 40 ± 2°C/75 ± 5% RH over 90 days are presented in Table 10. Physical integrity was maintained throughout. Hardness decreased marginally (5.8 → 5.2 kg/cm²), friability increased slightly (0.32% → 0.40%), and disintegration time extended modestly (7.2 → 7.8 min), all within pharmacopeial limits. Moisture content increased 1.10% → 1.30%, attributable to hygroscopic excipients under elevated humidity. Drug content of DFC (99.4% → 97.4%) and CTN (99.0% → 97.2%) remained within 90–110% LC throughout, confirming chemical stability. In-vitro release showed only a minor decrease (98.6% → 96.8% at 30 min), not clinically significant. These data support a projected 24-month room-temperature shelf life per ICH Q1A (R2) extrapolation [12].

Table 10. Accelerated stability data for optimised formulation F7 (40 ± 2°C / 75 ± 5% RH; ICH Q1A R2).

Parameter	Day 0	Day 30	Day 60	Day 90
Physical Appearance	Smooth, uniform, white	No visible change	Slight surface dullness; intact	Slight dullness; no cracks
Weight Variation (g)	1.89	1.88	1.87	1.86
Hardness (kg/cm²)	5.8	5.6	5.4	5.2
Friability (% w/w)	0.32	0.35	0.38	0.40
Disintegration (min)	7.2	7.4	7.6	7.8
Moisture Content (%)	1.10	1.18	1.24	1.30
DFC Content (% LC)	99.4	98.9	98.1	97.4
CTN Content (% LC)	99.0	98.6	97.8	97.2
In-vitro Release (% at 30 min)	98.6	97.9	97.3	96.8

Parameter	Day 0	Day 30	Day 60	Day 90
Overall Observation	Stable	Stable; no change	Within limits	Physically and chemically stable

DFC = diclofenac sodium; CTN = chondroitin sulphate; LC = label claim. All parameters within acceptance criteria throughout.

Discussion

This study presents the comprehensive RSM-guided development and evaluation of a triple-layer SR matrix tablet for co-delivery of CTN and DFC in OA—the first

published report of such a system. The novelty lies in the

triple-layer architecture providing bilateral polymer matrix protection, simultaneous modulation of two polymers via RSM, and co-delivery of a SYSADOA (CTN) and NSAID (DFC) in a single once-daily dosage form [14,16]. Drug–excipient compatibility, confirmed by DSC and FTIR, is a mandatory prerequisite for formulation stability. DSC studies showed partial amorphisation of both APIs in excipient mixtures (onset temperature reductions: CTN 148.81°C → 110.36°C; DFC 160.14°C → 111.25°C), which may enhance dissolution without chemical degradation, as no new exothermic decomposition peaks were observed [69]. FTIR analysis confirmed complete retention of all characteristic functional group absorptions for both APIs in excipient mixtures, providing unambiguous evidence of physicochemical compatibility [69]. These findings are consistent with established DSC and FTIR compatibility methodology for HPMC-based SR formulations [20,22,39]. Excellent pre-compression flow properties (angle of repose < 30°; CI < 11%; HR ≈ 1.11) across all nine formulations confirm that the wet granulation process produced uniform granule blends suitable for consistent tableting [71]. Post-compression evaluation confirmed all formulations met pharmacopeial standards for hardness (5.7–7.2 kg/cm²), friability (< 1%), weight variation (< ±5%), and drug content (85–115% LC) [72,74]. F7's highest drug contents (DFC: 98.02%; CTN: 98.95%) reflect superior mixing uniformity, critical for reliable therapeutic performance. In-vitro dissolution confirmed effective 12-hour SR for both APIs without burst release across all formulations. F7 produced the most balanced, reproducible dual SR (~98% CTN; ~95% DFC at 12 h), validating the triple-layer polymer architecture and the RSM-identified optimal concentration range [20,21,22,24]. The kinetic analysis unambiguously established non-Fickian anomalous transport (n = 0.5256–0.6968) with zero-order dominance—an ideal mechanism for chronic OA therapy maintaining near-constant plasma drug concentrations and minimising peak-trough fluctuations and dose-dependent GI adverse effects [13,16,39,75]. RSM optimisation was indispensable in mapping the complex, non-linear polymer concentration–response relationships. The quadratic model for %CDR (Adj. R^2 = 0.9997; F = 5375.91) identified HPMC K4M as the dominant rate-controlling excipient (~93.2% of model SS), entirely consistent with its high gel viscosity and established role as primary diffusional barrier in SR hydrophilic matrices [67]. Guar gum's smaller but significant positive contribution (F = 1021.73) reflects swelling-mediated matrix relaxation at moderate concentrations. The non-significant AB interaction confirms additive polymer behaviour, simplifying scale-up prediction [12,52]. The negative quadratic terms (A^2 and B^2) for both %CDR and %SI established that mid-range polymer concentrations are essential for optimal performance a critical finding achievable only by RSM and not by one-variable-at-a-time approaches [12]. This non-linearity directly justified the selection of F7's design space composition. Accelerated stability under ICH Q1A (R2) conditions confirmed F7's physicochemical robustness over 90 days. Minor increases in moisture content and disintegration time under 75% RH are expected for hygroscopic matrices and are pharmacologically inconsequential within Alu–Alu blistering [12]. These data support a 24-month room-temperature shelf life projection. Compared to previously reported SR DFC formulations using Hibiscus rosa-sinensis mucilage [21], Sesbania gum (71% release at 12 h) [22], and Eudragit RS PO blends (>70% at 7 h) [24], the present system provides superior dual-drug sustained control over 12 hours. The clinical rationale is compelling: CTN's chondroprotective effects [3,26,78] are sustained over 12 hours, and DFC's once-daily sustained delivery reduces GI mucosal exposure while maintaining anti-inflammatory efficacy [6,7,18,81]. The combination addresses both symptomatic and disease-modifying dimensions of OA in a single daily dosage form—directly improving patient adherence, which is critical in chronic OA management [10,13]. A limitation of the study is the absence of in-vivo pharmacokinetic data. Future studies should establish IVIVC, perform pilot-scale validation, and assess comparative bioavailability versus IR comparators in OA animal models.

Conclusion

This study successfully designed, RSM-optimised, and comprehensively evaluated a triple-layer hydrophilic

matrix tablet for the co-sustained oral delivery of chondroitin sulphate (300 mg) and diclofenac sodium (150 mg) for osteoarthritis management. The nine formulations prepared by wet granulation all satisfied pharmacopeial acceptance criteria for pre- and post-compression parameters, with drug–excipient compatibility confirmed by DSC and FTIR. The optimised formulation F7 (HPMC K4M 450 mg; guar gum 387.84 mg) demonstrated reproducible 12-hour dual sustained release governed by non-Fickian anomalous transport ($n = 0.6968$) with predominantly zero-order kinetics ($r = 0.9623$). RSM quadratic modelling identified HPMC K4M as the primary rate-controlling excipient (Adj. $R^2 = 0.9997$; $F = 5375.91$; $p < 0.0001$) and established mid-range polymer concentrations as essential for optimal %CDR and swelling behaviour. Accelerated stability studies confirmed physicochemical robustness over 90 days under ICH Q1A (R2) conditions. The triple-layer architecture delivers once-daily co-sustained release of CTN and DFC, integrating disease-modifying chondroprotective and anti-inflammatory pharmacology within a single scalable dosage form with substantially improved patient adherence potential and reduced GI adverse effect burden versus conventional IR regimens.

Declarations

Conflict of interest: The authors declare no conflict of interest.

Funding: This research received no specific grant from any funding agency in the public, commercial, or not-for-profit sectors.

Acknowledgements

The authors are grateful to the Management and Principal of JNTUA-Oil Technological and Pharmaceutical Research Institute, Anantapur, Andhra Pradesh, India, for providing the necessary facilities to carry out this research work.

References

1. Ruoslahti E. Structure and biology of proteoglycans. *Annu Rev Cell Biol.* 1988;4(1):229–255.
2. Liang PH, Wu CY, Greenberg WA, Wong CH. Glycan arrays: biological and medical applications. *Curr Opin Chem Biol.* 2008;12(1):86–92.
3. Lamari FN, Karamanos NK. Structure of chondroitin sulfate. *Adv Pharmacol.* 2006;53:33–48.
4. Uebelhart D. Clinical review of chondroitin sulfate in osteoarthritis. *Osteoarthritis Cartilage.* 2008;16(Suppl 3):S19–S21.
5. Miller KL, Clegg DO. Glucosamine and chondroitin sulfate. *Rheum Dis Clin North Am.* 2011;37(1):103–118.
6. Schmidt M, Sørensen HT, Pedersen L. Diclofenac use and cardiovascular risks: series of nationwide cohort studies. *BMJ.* 2018;362:k3426.
7. Díaz-González F, Sánchez-Madrid F. NSAIDs: learning new tricks from old drugs. *Eur J Immunol.* 2015;45(3):679–686.
8. Carvalho FR, Queiroz VF, Gavaia PJ. Exploring novel biomarkers for early detection of osteoporosis. *medRxiv.* 2025 May 31. doi:10.1101/2025.05.29.25328628.
9. García Rodríguez LA, Egan K, FitzGerald GA. Traditional NSAIDs and postmenopausal hormone therapy: a drug–drug interaction? *PLoS Med.* 2007;4(5):e157.
10. Prakhar A, Semimul A. A comprehensive review on sustained release matrix tablets: a promising dosage form. *Univ J Pharm Res.* 2018;3(5):1–10.
11. Mastropietro DJ, Park K, Omidian H. Polymers in oral drug delivery. In: *Comprehensive Biomaterials II*, Vol. 4. Elsevier; 2017.
12. Sopyan IY, Gozali DO, Kurniawansyah IS, Guntina RK. Design-Expert software (DOE): an application tool for optimisation in pharmaceutical formulation. *Int J Appl Pharm.* 2022;14(4):55–63.
13. Zalte HD, Saudagar RB. Review of the sustained-release matrix tablet. *Int J Pharm Biol Sci.* 2013;3(4):17–29.
14. Bisht T, Rishiwer P, Kumar P. Review on matrix tablet. *Indo Global J Pharm Sci.* 2016;4(6):1–10.
15. Cardinal JR. Drug release from matrix devices. In: *Recent Advances in Drug Delivery Systems.* Plenum Press; 1984:229–248.
16. Mondal N. The role of the matrix tablet in the drug delivery system. *Int J Appl Pharm.* 2018;10(1):1–6.
17. Solate JT. *Dictionary of Pharmaceutical Dosage Forms.* CRC Press; 2020.
18. Brogden RN, Heel RC, Pakes GE, Speight TM, Avery GS. Diclofenac sodium: a review of its pharmacological properties and therapeutic use. *Drugs.* 1980;20(1):24–48.
19. Ramasamy T, Khandasamy US, Shanmugam S, Ruttala H. Formulation and evaluation of chondroitin sulphate tablets of aceclofenac for colon-targeted delivery. *Iran J Pharm Res.* 2012;11(2):465–476.
20. Sahu P. Evaluation of sustained release matrix tablets using natural polymers. *Int J Pharmacogn Herb Drug Technol.* 2025;2(4):14–25.

21. Ahad HA, Suresh Kumar C, Yesupadam P, Sandhya Rani P, Chandra Sekhar A, Sivaramakrishna GV. Designing and evaluation of diclofenac sodium sustained release matrix tablets using *Hibiscus rosa-sinensis* leaves mucilage. *Int J Pharm Sci Rev Res.* 2010;1(2):29–31.
22. Vasaikar RS, Chatap VK, Jain P, Bhat MR. Formulation and characterisation of diclofenac sodium matrix tablets using Sesbania gum as a novel carrier. *Acta Biomed.* 2023;94(1):e2023007.
23. Sanni G, Santosh K. Formulation and evaluation of a combined dosage form of diclofenac sodium (mini tablet) and omeprazole sodium in capsule devices. *J Pharm Res Sci Technol.* 2022;6(1):162.
24. Eraga SO, Ijeh LN, Nnamani ND, Eichie FE. Formulation of sustained-release diclofenac sodium tablets using a blend of hydrophobic and hydrophilic polymers. *Drug Discov.* 2023;17:e12dd1013.
25. Volpi N, Maccari F. Quantitative and qualitative evaluation of chondroitin sulfate in dietary supplements. *Food Anal Methods.* 2008;1(3):195–204.
26. Ashruf OS, Ansari MY. Natural compounds: potential therapeutics for inhibition of cartilage matrix degradation in osteoarthritis. *Life.* 2022;13(1):102.
27. Bustos Araya ME, Nardi-Ricart A, Calpena Capmany AC, Miñarro Carmona M. Chondroitin sulfate for cartilage regeneration administered topically using a nanostructured formulation. *Int J Mol Sci.* 2024;25(18):10023.
28. Erenler AS, Unver T, Melekoglu R. Assessment of the antifungal effect of microbial chondroitin sulfate against predominant *Candida* strains. *Iran J Chem Chem Eng.* 2024;43(5):1–10.
29. Shen Q, Guo Y, Wang K, Zhang C, Ma Y. A review of chondroitin sulfate's preparation, properties, functions, and applications. *Molecules.* 2023;28(20):7093.
30. Qaiser R, Pervaiz F, Hanan H, Shoukat H, Nadeem M. Chondroitin sulfate-based mucoadhesive interpenetrating polymeric hydrogels of captopril. *Polym Bull.* 2024;81(6):5267–5293.
31. Agale KA, Shinde SP. A review on floating tablet. *J Drug Deliv Ther.* 2025;15(2):1–8.
32. Howard MT, Klinzing GR. Effects of dwell time and loading strain rate on powder compaction and tablet properties. *Powder Technol.* 2025;453:120759.
33. Ge Y, Yuan Z, Zhang M, et al. Direct compression tablet formulation of trimetazidine through systematic screening of oxalate salts. *Int J Pharm.* 2025;669:125255.
34. Patel SK, Prathyusha S, Kasturi M, et al. Optimising Irbesartan fast dissolving tablets using natural polysaccharides. *Int Res J Multidiscip Scope.* 2025;6(1):1181–1190.
35. Özok Hİ, Keskin E, Yardım Y. Voltammetric procedure for sensing liothyronine sodium in tablet dosage form using boron-doped diamond electrode. *Diamond Relat Mater.* 2025;152:112078.
36. Pflieger T, Venkatesh R, Dachtler M, Laufer S, Lunter D. Drug release kinetics of 3D-printed two-compartment theophylline and prednisolone tablets. *Int J Pharm.* 2025;669:125218.
37. Zhang W, Thool P, Weitz BW, Hou HH. Effects of formulation variables on disintegration of spray-dried amorphous solid dispersion tablets. *J Pharm Sci.* 2025;114(1):304–312.
38. Lü Y, Li P, Xu L, Zh Y, Zh C. Preparation of calcium citrate malate granules and their application in tablet formulation. *China Food Addit.* 2025;36(1):1–9.
39. Patra R, Mishra P, Pani MK, Parida L, Mishra S. Development and characterisation of lornoxicam sustained release tablets using HPMC K4M. *J Drug Deliv Ther.* 2025;15(3):1–8.
40. Amrutkar JR, Gattani SG. Chitosan–chondroitin sulfate-based matrix tablets for colon-specific delivery of indomethacin. *AAPS PharmSciTech.* 2009;10(2):670–677.
41. Zhou J, Yi T, Zhang Z, et al. Electrospun Janus core (EC//PEO)@shell (HPMCAS) hybrids for colon-targeted drug absorbance. *Adv Compos Hybrid Mater.* 2023;6(6):189.
42. Yuvasree V, Umasankar K. A review: colon targeted drug delivery system. *Pharm Res.* 2024;14(01):1–12.
43. Arévalo-Pérez R, Maderuelo C, Lanao JM. Development of intestinal colonic drug delivery systems for diverticular disease: a QbD approach. *Eur J Pharm Sci.* 2024;203:106918.
44. Doggwiler V, Gazzaniga A, Cerea M, Kleinebudde P. Mechanisms underlying drug release from controlled colonic release tablet based on xyloglucan polysaccharide matrix. *J Control Release.* 2024;370:512–523.
45. Gunawan M, Salim N, Elim D. Polysaccharides and polymers as excipients in colon-targeted drug delivery systems. *Int J Pharm Pharm Sci.* 2025;17(2):1–10.
46. Mamatha V, Rao P, Naidu R. Effect of chitosan and sodium alginate on release rate of levetiracetam for extended-release formulations. *Asian J Pharm Clin Res.* 2025;18(3):45–52.
47. Tanpure S, Pawar J, Dixit G. Development and optimisation of bilayer matrix tablets of

losartan potassium using plant-derived polymers. *Int J Pharm Sci Drug Res.* 2025;17(1):1–9.
48. Lee J, Kim Y, Park S. Reflection-based THz-TDS for simultaneous tablet thickness and porosity determination. *J Pharm Sci.* 2025;114(4):1782–1790.
49. Nausheen A, Khan M, Hussain M. Formulation and evaluation of dexlansoprazole floating tablets. *Pak J Pharm Sci.* 2025;38(2):301–310.
50. Nurhayati L, Suharto B, Fauziyah S. Nanocellulose-coated activated carbon tablets for controlled bacterial release. *Int J Pharm.* 2025;671:125340.
51. Viachou M, Stavros P, Nikolaos T. Novel branched polylactide-based melatonin tablet formulations. *Eur J Pharm Biopharm.* 2025;198:114268.
52. Jaimini R, Jaimini M. Formulation and optimization of gastro-retentive floating tablets of enalapril maleate and losartan for enhanced bioavailability and therapeutic efficacy. *Trop J Pharm Life Sci.* 2025;12(1):01–10.
53. Mirgal S, Kadam V, Bhosale S. Gastro-effervescent tablets: formulation, development, and evaluation. *J Drug Deliv Ther.* 2025;15(4):1–8.
54. Lakkakula S, Reddy S, Kiran U. Gastroretentive non-effervescent floating matrix formulation of cefaclor using HPMC grades. *Asian J Pharm.* 2025;19(1):1–9.
62. Amidon S, Brown JE, Dave VS. Colon-targeted oral drug delivery systems: design trends and approaches. *AAPS PharmSciTech.* 2015;16(4):731–741.
63. Srikar G, Kalyani P, Padmavathi K. Dextrin as a binder in colon-specific matrix tablets: formulation and evaluation. *J Pharm Res.* 2013;6(3):321–326.
64. Sopyan I, Muchtarudi M. Targeted drug delivery to the colon: approaches and evaluation. *J Adv Pharm Technol Res.* 2023;14(1):1–12.
65. Sharma R, Mehta M, Panda S. Chondroitin sulphate as a biomaterial for drug delivery and tissue engineering. *J Drug Deliv Sci Technol.* 2022;67:103053.
66. Patel DM, Patel CN. Formulation and evaluation of atenolol sustained release matrix tablets using various polymers. *Int J Pharm Investig.* 2012;2(1):26–32.
67. Nokhodchi A, Raja S, Patel P, Asare-Addo K. The role of oral controlled release matrix tablets in drug delivery systems. *Bioimpacts.* 2012;2(4):175–187.
68. Kannan K, Manikandan M, Manavalan R, Valliappan K. Formulation and evaluation of fexofenadine sustained release matrix tablets
55. Khaire O, Deshmukh S, Pore Y. Transferrin-tagged rivastigmine microspheres for Alzheimer's disease using Box–Behnken design. *AAPS PharmSciTech.* 2025;26(3):1–12.
56. González-Rodríguez ML, Maestrelli F, Mura P, Rabasco AM. In vitro release of sodium diclofenac from a central core matrix tablet aimed for colonic drug delivery. *Eur J Pharm Sci.* 2003;20(2):125–131.
57. Jeganathan B, Shanmugam S, Sethuraman S. Polyelectrolyte multilayer film (EE/HPMCAS) for pH-dependent sustained diclofenac release. *Int J Pharm.* 2016;514(1):135–144.
58. Ashraf MU, Hasan MM, Sharif S, Murtaza G. Seed hydrogel for sustained release tablets of theophylline and diclofenac sodium. *Polym Bull.* 2018;75(9):4265–4285.
59. Zhao L, Guo J, Li Y, Liu Y, Xu FJ. Chondroitin sulfate-based nanocarriers for drug/gene delivery. *Biomaterials.* 2015;35(24):6395–6407.
60. Jose S, Dhanya K, Cinu TA, Aleykutty NA. Oral colon-targeted drug delivery: past, present, and future. *J Pharm Sci.* 2009;12(1):1–12.
61. Ramu B, Sundhararajan M, Mary SA. Formulation and evaluation of colon-specific press-coated tablets of lansoprazole. *Int J Pharm Pharm Sci.* 2015;7(5):261–266.

using HPMC K15M. *Int J Pharm Tech Res.* 2010;2(2):1361–1369.
69. Indian Pharmacopoeia Commission. *Indian Pharmacopoeia 2022.* Vol. I. Ghaziabad: IPC; 2022. [Preformulation evaluation methods.]
70. Montgomery DC. *Design and Analysis of Experiments.* 8th ed. Wiley; 2013. [RSM optimisation of polymer concentrations.]
71. Carr RL. Classifying flow properties of solids. *Chem Eng.* 1965;72:163–168.
72. Indian Pharmacopoeia Commission. *Indian Pharmacopoeia 2022.* Vol. II. Ghaziabad: IPC; 2022.
73. British Pharmacopoeia Commission. *British Pharmacopoeia 2023.* London: HMSO; 2023.
74. United States Pharmacopeia and National Formulary (USP 45–NF 40). Rockville, MD: USP; 2022.
75. Korsmeyer RW, Gurny R, Doelker E, Buri P, Peppas NA. Mechanisms of solute release from porous hydrophilic polymers. *Int J Pharm.* 1983;15(1):25–35.
76. Chondroitin sulfate monograph. *European Pharmacopoeia* 11th Ed. Strasbourg: EDQM; 2023.
77. Volpi N. Chondroitin sulphate: structure, role and pharmacological activity. *Adv Pharmacol.* 2006;53:81–258.

78. Clegg DO, Reda DJ, Harris CL, et al. Glucosamine, chondroitin sulfate, and the two in combination for painful knee osteoarthritis. *N Engl J Med.* 2006;354(8):795–808.
79. Volpi N. Oral bioavailability of chondroitin sulfate and its constituents. *Osteoarthritis Cartilage.* 2009;17(Suppl 1):S26–S27.
80. ICH Harmonised Tripartite Guideline. Stability testing of new drug substances and products Q1A(R2). International Council for Harmonisation; 2003.
81. Brogden RN, McTavish D. Diclofenac sodium: an appraisal of its pharmacodynamic and pharmacokinetic properties. *Drugs.* 1990;40(2):240–258.